



National Institute of Oceanography and Fisheries
Egyptian Journal of Aquatic Research

<http://ees.elsevier.com/ejar>
www.sciencedirect.com



FULL LENGTH ARTICLE

Late Holocene hydrographic settings of the northern Red Sea



Amani Badawi

National Institute of Oceanography and Fisheries, Al-Anfushi 21556, Alexandria, Egypt

Received 22 July 2015; revised 8 September 2015; accepted 8 September 2015

Available online 10 October 2015

KEYWORDS

Northern Red Sea;
 Paleo-oceanography;
 Surface water salinity;
 Late quaternary hydro-
 graphic conditions;
 Planktonic foraminifera

Abstract Temporal variability of the paleo-oceanographic setting of the northern Red Sea during the last 6 Ky was deduced from high-resolution faunal results and stable isotope records of planktonic foraminifera in three short cores sediment obtained by the German R/V Meteor vessel. In general, the investigated time interval is fundamentally comparable to the present day composition and distribution of planktonic foraminifera. However, interrupted short enhanced arid phase spanning the last 4–2 Ky appears to have existed in the northern Red Sea, and resulted in elevation of salinity and somehow productivity, as hypersaline, dense surface water favored vertical mixing of the water column resulting in an increase in productivity. This paleoclimatic reconstruction is revealed from the distinct gradient in the composition and distribution of planktonic foraminifera, as well as the significant distribution trend of *Globigerinoides ruber* versus *Globigerinoides sacculifer* correlated with the stable isotope records. Starting from the last 2 Ky to the present time, less strength arid conditions relative to the previous period prevailed, reflected from a gradual decrease in surface water salinity and productivity assuming that the present water conditions and consequently current climatic conditions began to develop from that time with minor fluctuations reaching the recent conditions.

© 2015 National Institute of Oceanography and Fisheries. Hosting by Elsevier B.V. This is an open access article under the CC BY-NC-ND license (<http://creativecommons.org/licenses/by-nc-nd/4.0/>).

Introduction

Mediterranean climate is influenced the Red Sea by seasonal wind systems (NNW winds) from the north, as well as the African and Arabian monsoon systems (SSE winds) from the south. The pattern and wind magnitude are strong factors over the Red Sea region represented by two wind systems. During summer, (June–August), the prevailing NNW winds blow throughout the basin. During winter, (September–May), the

NNW winds are restricted to the northern region, allowing the SSE winds, corresponding to seasonal changes of the Arabian monsoon system, to influence the southern region resulting in a convergence zone around 19°N (Patzert, 1974; Eshel et al., 1994; Hamouda and El-Wahab, 2009, 2012). Surface and subsurface water masses circulation of the Red Sea is controlled by the seasonal wind system. During summer, a three-layer current system is generated, driven by NNW winds. Northern Red Sea surface water propagates into the Gulf of Aden, at the same time, nutrient-rich intermediate water proceeds northward as subsurface matter mass (Eshel and Naik, 1997; Smeed, 2004) while the third deep water layer outflows the highly-saline water mass from the northern Red

E-mail address: amani_badawi@yahoo.com

Peer review under responsibility of National Institute of Oceanography and Fisheries.

<http://dx.doi.org/10.1016/j.ejar.2015.09.001>

1687-4285 © 2015 National Institute of Oceanography and Fisheries. Hosting by Elsevier B.V.

This is an open access article under the CC BY-NC-ND license (<http://creativecommons.org/licenses/by-nc-nd/4.0/>).

Sea southward into the Gulf of Aden (Bower and Furey, 2012). During winter, winds over the southern Red Sea reverse and generate a two-layer current pattern. The surface water of Gulf of Aden (with normal salinity, $\sim 37\text{‰}$) flows northward into the Red Sea through the Strait of Bab el Mandeb, and it moves northward in more arid to semi-arid conditions. Extreme evaporation occurs leading to an increase in salinity to about 40‰ and density, permitting the formation of deep water during winter at the northern Red Sea (Edwards, 1987). Red Sea deep hypersaline water outflows southward into the Gulf of Aden and its renewal is regulated by seasonal deep-water formation during winter at the Gulf of Suez (average depth of 50 m) where a warm, highly saline, dense surface water sinks to deeper depths forming a warm ($21.6\text{--}21.8\text{ }^{\circ}\text{C}$) and saline ($40.5\text{--}40.6\text{‰}$) intermediate and deep-water masses that extend southward and ventilate the Red Sea deep water (Cember, 1988; Woelk and Quadfasel, 1996). In addition to this, there is a minor annual contribution of Gulf of Aqaba water (Edwards, 1987; Eshel and Naik, 1997).

Several studies on stable oxygen and carbon isotopes of planktonic and benthonic foraminifera from the Red Sea revealed the detailed picture of water mass variation with association of global climatic changes during the Late Pleistocene and Early Holocene (e.g. Almogi-Labin et al., 1996; Ivanova, 1985; Locke and Thunell, 1988; Hemleben et al., 1989, 1996; Fenton et al., 2000; Siddall et al., 2003, 2004; Badawi, 2015; Badawi et al., 2005; Hamouda, 2009; Siccha et al., 2009; Abu-Zied et al., 2013). Individual species of planktonic foraminifera characterized by distinct ecological preferences and tolerance regarding temperature, salinity and productivity as well as biological lifestyles help in quaternary stratigraphy and paleoenvironmental reconstructions (Vincent and Berger, 1981; Kroon and Ganssen, 1989; Ravelo and Fairbanks, 1992, 1995; Rohling et al., 2004; Schiebel and Hemleben, 2005; Farmer et al., 2007; Edelman-Fürstenberg et al., 2009; Birch et al., 2013). The objective of this study is to investigate the abundance, distribution and stable isotope records of planktonic foraminifera in Late Holocene deep-sea short sediment cores recovered from the northern Red Sea and link these with climatic changes in the Red Sea during this interval.

Materials and methods

Three short sediment cores from the deep-sea bottom sediments of the northern Red Sea were obtained by the German R/V Meteor-Cruise, Leg M 31/2, (February 1995), between latitudes $25^{\circ}31.3'$ and $27^{\circ}41.2'N$ (Fig. 1). The northern core MC 78 was collected at $27^{\circ}41.200'N$, $34^{\circ}35.800'E$, 1018 m water depth, with a core recovery of 27 cm. The central core MC 361 was collected at $25^{\circ}44.982'N$, $34^{\circ}52.065'E$, 720 m water depth, with a core recovery of 29 cm. The southern core MC 86 was collected at $25^{\circ}31.300'N$, $35^{\circ}36.500'E$, 941 m water depth, with a core recovery of 28.5 cm.

Sediment cores were sliced into sediment samples every 0.5 and 1 cm intervals. From each sample, about 5 g of wet sediment was dried, weighed, disintegrated with H_2O_2 (3.5%), and washed through a 30 mm mesh sieve. The residue was oven-dried at $40\text{ }^{\circ}\text{C}$. Subsequently, the samples were dry sieved into the fractions $<125\text{ }\mu\text{m}$, $125\text{--}250\text{ }\mu\text{m}$, and $>250\text{ }\mu\text{m}$, then weighed again. The fractions $125\text{--}250\text{ }\mu\text{m}$ and $>250\text{ }\mu\text{m}$ were investigated for their planktonic foraminiferal content.

Planktonic foraminifera were identified according to Loeblich and Tappan (1988) and counted using a binocular microscope. Then, they were normalized to 1 g of dry sediment. Relative abundance was calculated to facilitate the comparison of the data sets providing percentage curves of the most frequent species. Relative abundance of all planktonic foraminiferal shell counts was conveyed by normalizing the number of each individual species relative to the total number of all identified species in each sample. Rare species that have relative abundance below of 0.5% or recorded in one sample have been skipped from the data set (Malmgren and Haq, 1982; Schmiedl et al., 1998). For stable isotope measurements of core MC 78, 15–20 tests of tropical–subtropical planktonic foraminiferal species *Globigerinoides ruber* and *Globigerinoides sacculifer* were picked from the $>250\text{ }\mu\text{m}$ fraction. Prior to analysis, selected tests were ultrasonically cleaned in a bath of warm water. The isotope measurements were carried out at the Department of Geosciences, Bremen University, Germany.

Results

Age model of the investigated cores

Sediment cores stratigraphy is developed based mainly on the graphical correlation of the measured stable oxygen isotope data of core MC 78 with the global SPECMAP $\delta 18\text{O}$ curve (Imbrie et al., 1984). The estimated age model of the Holocene section of core MC 78 (Fig. 2), is assumed to cover the last 6 Ky based on 14C data set of other cores in the Red Sea provided through personal communication with Ch. Hemleben, Tuebingen University, Germany. In addition, the resulting age model, sedimentation rate, and faunal pattern of the core MC 78 are in good agreement with published data of Red Sea core (Badawi et al., 2005; Siccha et al., 2009). The three studied cores can be stratigraphically correlated with each other, and the age model of MC 78 could be extrapolated to the other two investigated cores MC 361 and MC 86, where the maximum horizontal separation distance being $\sim 234\text{ km}$.

As such, they are belonging to the same basinal structures and stratigraphical setting, in which deposition is relatively continuous and uniform, with more or less limited variation in the average sedimentation rate for a short period.

Stable isotope signals

The stable isotope profiles of the index species *G. ruber* and *G. sacculifer* in the core MC 78 slightly fluctuate throughout the core. In general, the $\delta 18\text{O}$ of *G. ruber* is lighter than that of *G. sacculifer*. The amplitude of *G. ruber* signal throughout the core ranges between -0.83‰ and -0.03‰ . The $\delta 18\text{O}$ of *G. sacculifer* ranges between -0.11‰ and 0.90‰ (Fig. 3). The $\delta 18\text{O}$ of *G. ruber* and *G. sacculifer* show relatively heavy values during the interval from about 4 to 2 Ky BP with an average value of -0.3 and 0.3 , respectively (Fig. 3). The carbon isotope records of *G. sacculifer* and *G. ruber* exhibit two different values. *G. sacculifer* displays generally heavy values during the last 6 Ky BP, whereas the $\delta 13\text{C}$ curve of *G. ruber* shows a similar trend to that of *G. sacculifer* but in a much more irregular way. The $\delta 13\text{C}$ amplitude of the *G. ruber* varies between 1.12‰ and 1.87‰ and *G. sacculifer* varies between 2.19‰ and 2.86‰ (Fig. 3). Planktonic foraminifera.

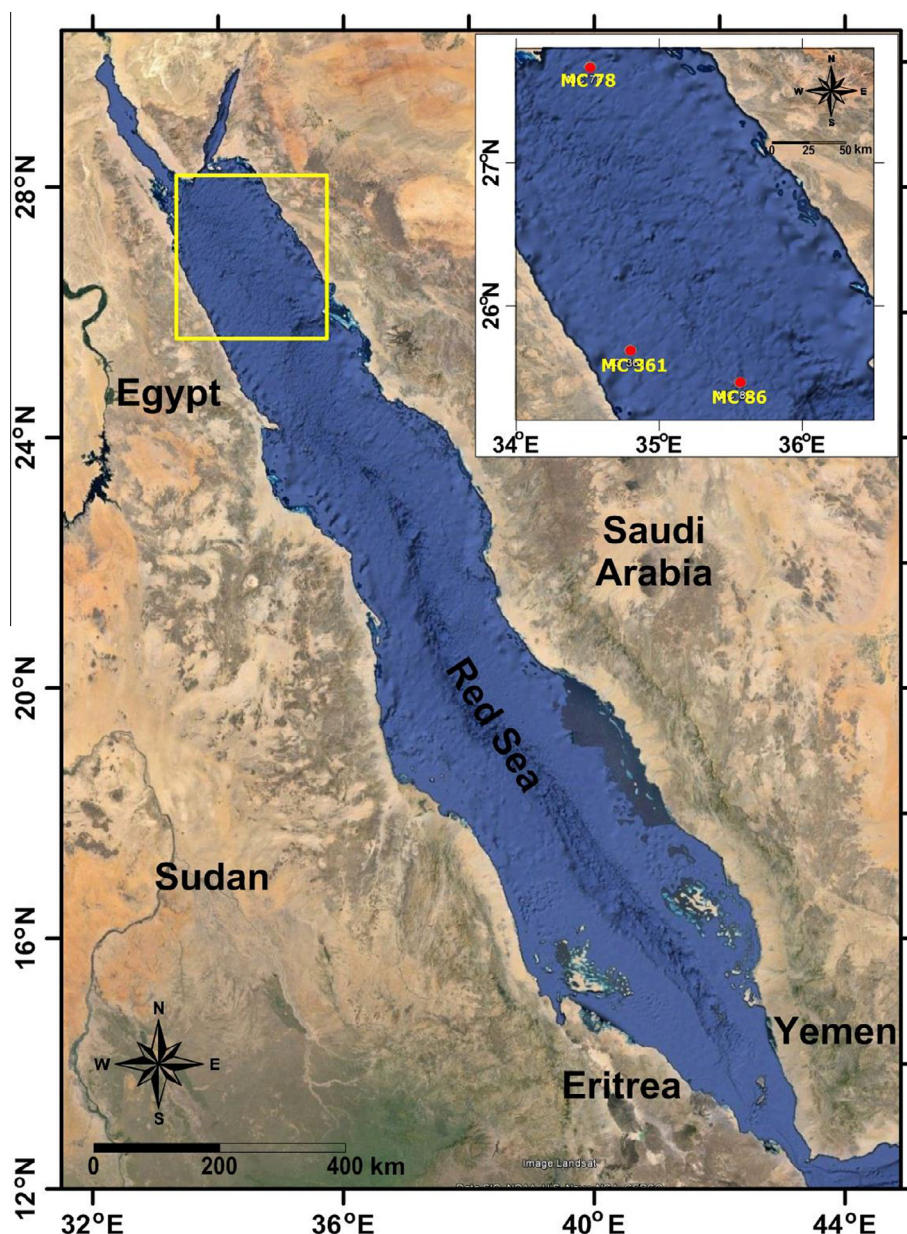


Figure 1 Location of the study area. The studied core sites are indicated by solid circles.

The most common planktonic foraminiferal species that occur in the sediments ($> 250 \mu\text{m}$) of the studied cores are *G. sacculifer*, *G. ruber*, *Globigerinella siphonifera*, and *Orbulina universa*. Other species occur, but with low frequency such as *Globigerinoides conglobatus*, *Globigerinoides calida*, *Globigerinoides aequilateralis* and *Hastigerina pelagic*. In the $125\text{--}250 \mu\text{m}$ fraction, five different species were identified, forming un-appreciable part of the total fauna such as *Globigerina quinqueloba*, *Globorotalia anfracta*, *Globigerinoides rubescens*, *Globigerineta glutinata*, *Globigerineta tenella*. All of these species were also recorded in the $> 250 \mu\text{m}$ fraction. The relative abundance of the four dominant species of planktonic foraminifera (*G. sacculifer*, *G. ruber*, *G. siphonifera*, and *O. universa*) in the $> 250 \mu\text{m}$ fraction and varying throughout the studied three cores is presented in Fig. 4. From about 6–4 Ky BP, in the Core MC 78, *G. sacculifer* is the most

abundant species with relative abundance of 19–54%, followed by *O. universa* (19–42%), *G. siphonifera* (18–27%), and *G. ruber* (9–20%). For the same interval, in the Core MC 361, *G. sacculifer* increases to 71%, reaching its maximum abundance of 81% at the end of the core.

G. ruber, *G. siphonifera*, and *O. universa* exhibit the same decreasing trend, displaying relative abundances of 6–16%, 4–10% and 5–9%, respectively (Fig. 4). Almost same trends of species distribution are recorded in the Core MC 86 where *G. sacculifer* is the most abundant species representing 57–77% of the total fauna. The percentage of *G. ruber*, *G. siphonifera*, and *O. universa* is very low and almost constant from 5% to 10%, 8% to 17% and 6% to 18%, respectively. In the interval from ~4 to 2.5 Ky BP of the Core MC 78, the relative abundance of *G. sacculifer* exhibits a sharp decline to 9–16%, while *G. ruber* reaches its maximum abundance

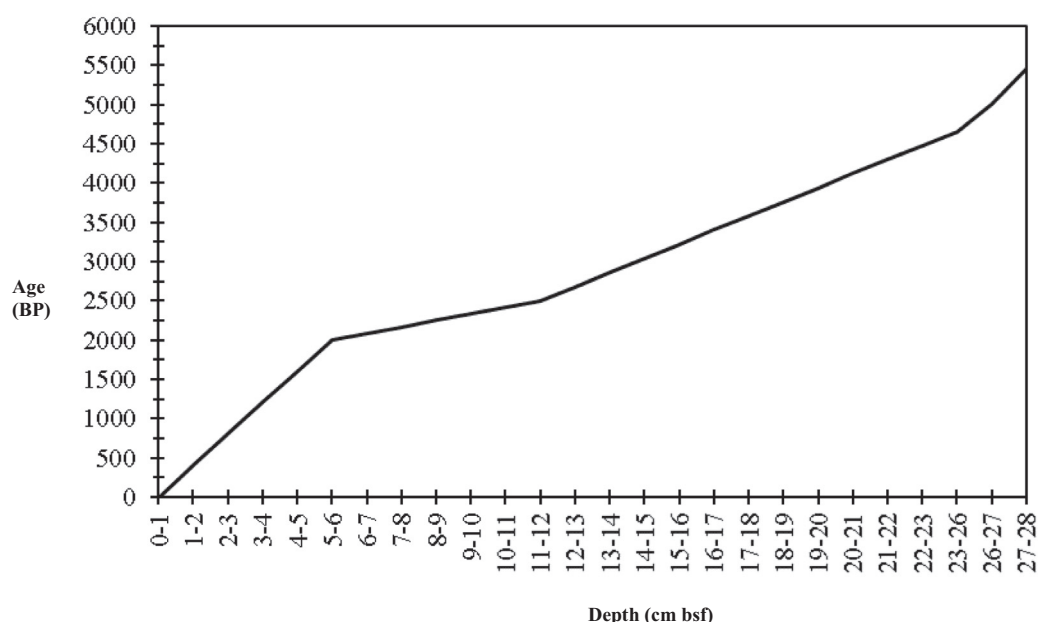


Figure 2 Age model of the northern Red Sea core, MC 78. Core depth below sea floor (cm bsf) is plotted against estimated age.

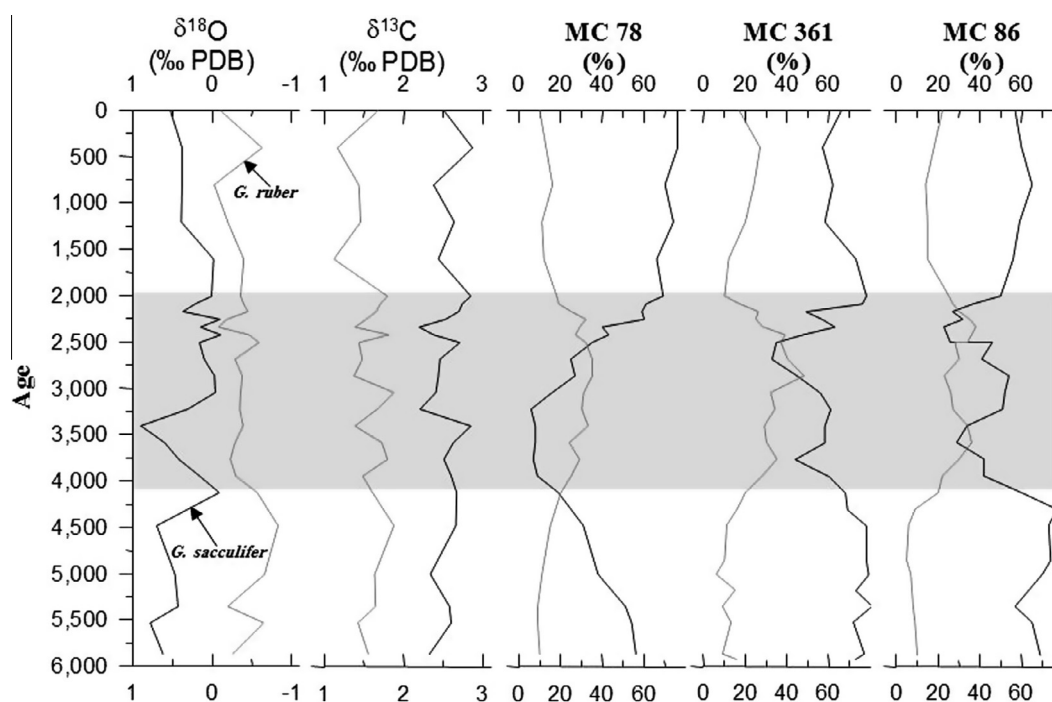


Figure 3 Oxygen and carbon stable isotopes of *G. sacculifer* and *G. ruber* in core MC 78. They were plotted against age and correlated with the same species in cores MC 361 and MC 86, northern Red Sea.

(24–33%) throughout the same interval (Fig. 4). *G. siphonifera* and *O. universa* also show marked increases during this interval ranging between 19–28% and 31–44%, respectively. Faunal distribution in the Core MC 361 and MC 86 follows almost the same general trend of the MC 78 fauna. The relative abundance of *G. sacculifer* decreases gradually to reach 30% and 63% of the total fauna. *G. ruber*, *G. siphonifera* and *O. universa* show an increasing trend with relative abundances

of 25–40%, 4–9% and 11–30%, respectively. In the core MC 86, the distribution pattern of *G. ruber*, *G. siphonifera*, and *O. universa* begins to increase gradually with abundances of 22–38%, 8–16% and 11–33%, respectively whereas, *G. sacculifer* decreases gradually from 54% to 23%. A very short transition interval has been noticed at ~2.5–2 Ky BP in the three cores. This interval is characterized by increases in *G. sacculifer* from 27% to 60%. *G. ruber*, *G. siphonifera*,

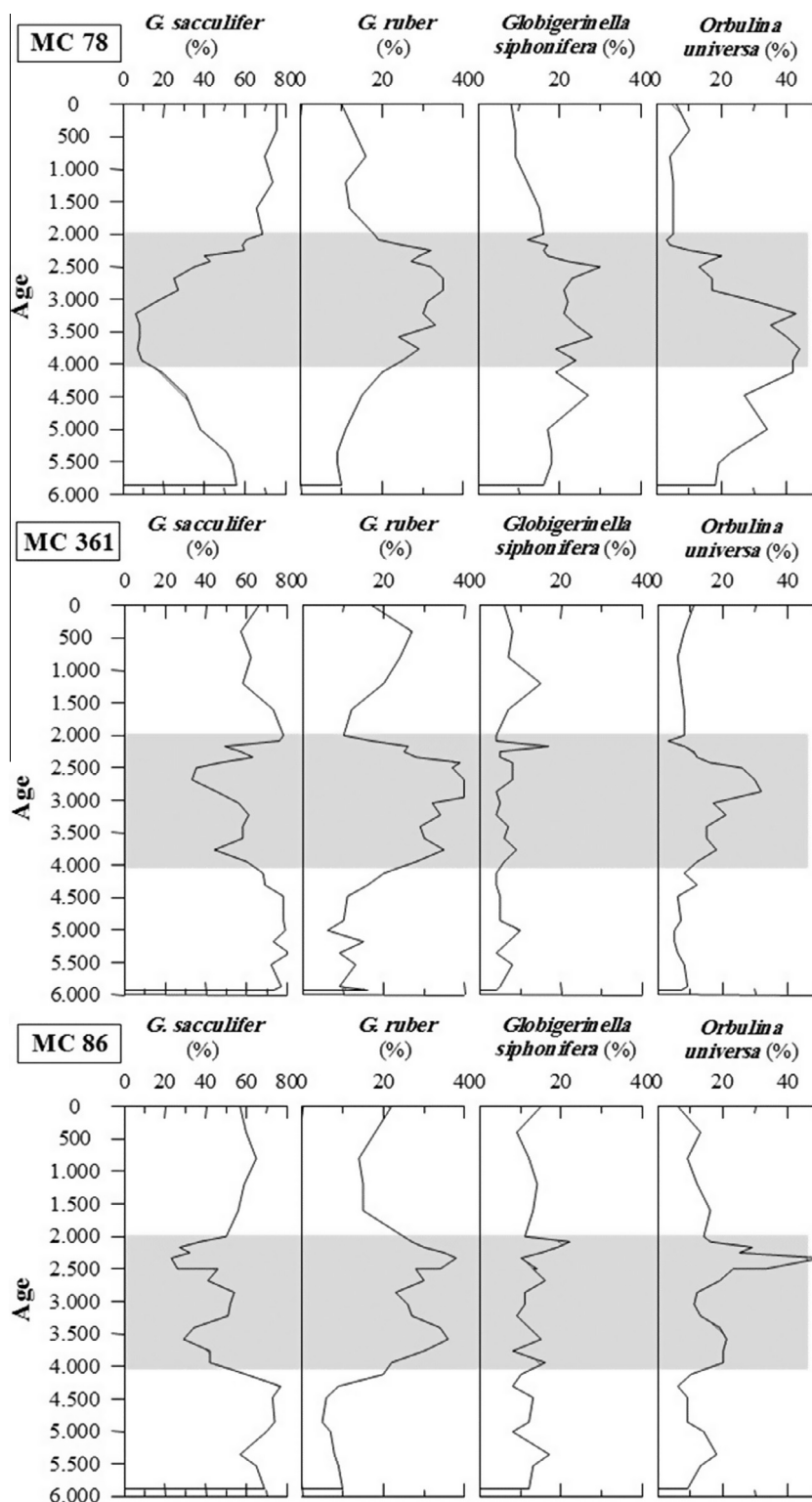


Figure 4 Relative abundance (%) of the four dominant species (*G. sacculifer*, *G. ruber*, *G. siphonifera* and *O. universa*) in the cores MC 78, MC 361 and MC 86, northern Red Sea.

and *O. universa* account for 20–35%, 16–21%, and 10–17% of the total faunal assemblages, respectively (Fig. 4). In the last 2 Ky BP, *G. sacculifer* is the most common species (Fig. 4). In the core MC 78, the relative abundance of *G. sacculifer* (59–76%), dominates the occurrence of *G. ruber*, while the

relative abundance of *G. ruber*, *G. siphonifera*, and *O. universa* recorded between 10–25%, 8–17%, and 3–10%, respectively. In the core MC 361, the relative abundance of *G. sacculifer* ranges from 57% to 78% while *G. ruber* ranges from 10% to 27%. *G. siphonifera* and *O. universa* ranges from 4% to 15%

and 3% to 11%, respectively. In Core MC 86, *G. sacculifer* also dominates with abundance ranging from 50% to 65%.

G. ruber ranges from 14% to 25%. *G. siphonifera* and *O. universa* range from 9% to 15 and 6% to 16%, respectively.

Discussion

Paleo-oceanographic setting

The stable isotopes of *G. sacculifer* and *G. ruber* shells combined with other planktonic foraminiferal species abundance and distribution provide a good picture of their ecosystem through time in the studied cores. In the studied cores, typical warm tropical/subtropical planktonic foraminiferal fauna has been detected in the sediment samples of the studied three northern Red Sea cores, showing remarkable variations in abundance and distribution. In tropical/subtropical region, mainly two species (*G. sacculifer* and *G. ruber*) have been used as paleoclimatic indicators (e.g. Berggren and Boersma, 1969; Bé and Tolderlund, 1971; Vincent and Berger, 1981). The relative abundance of the two index species (*G. sacculifer* and *G. ruber*) versus time along the investigated cores, (Fig. 3) shows an inverse relationship throughout the studied cores. The distribution of *G. siphonifera* and *O. universa* follows almost the same trend as *G. ruber*. Generally, the dominance of low-diversity planktonic foraminiferal assemblages of the northern Red Sea is characterized by *spinose*, *symbiont-bearing*, and *epipelagic species*. While the southern Red Sea and Gulf of Aden assemblages, showed highest frequencies of the *non-spinose species Globorotalia menardii* and *Neogloboquadrina dutertrei* (Schundnagies et al., 1990). These north–south differences have been attributed mainly to relevant gradients in salinity and trophic conditions.

Evaluation of paleo-surface water temperature

The continuous abundance of the four dominant planktonic foraminiferal species *G. ruber*, *G. sacculifer*, *G. siphonifera* and *O. universa* in the present investigated cores, indicates that water temperature during the last 6 Ky BP, had a minimum value of approximately 18 °C (Berggren and Boersma, 1969; Bé and Tolderlund, 1971). A wide range of tolerance to the temperature of *G. ruber* and *G. sacculifer* (16–31 °C and 14–31 °C, respectively) shows that their distribution could not have been controlled by temperature alone. Salinity and productivity might mask the effect of temperature. In addition *G. sacculifer*, *G. ruber*, *G. siphonifera* and *O. universa* can also be considered as indicators of warm waters and recent seasonal variation in temperature and salinity. They withstand the temperature of 12–31 °C and 11–30 °C, respectively (Reiss et al., 1980; Almogi-Labin et al., 1996; Hemleben et al., 1989).

Evaluation of paleo-surface water salinity

The last 6 Ky BP is characterized by fluctuation in percentages of various identified species, which could reflect salinity variations of the water masses during this time interval. In the studied cores, salinity tolerance of *G. ruber*, *G. sacculifer*, *O. universa* and *G. siphonifera* is 22–49‰, 24–47‰, 23–46‰ and 27–45‰, respectively (Lipps, 1979; Hemleben et al.,

1989; Bijma et al., 1990). At the beginning of 6 Ky BP, the salinity is suggested to be high with the gradual increase to reach its optimum extreme value through the period 4–2 Ky BP. This interval is characterized by increasing trend in relative abundance of *G. ruber*, the most flexible species among planktonic foraminifera, which has wide salinity tolerance, at the expense of *G. sacculifer* and its relative abundance decreased accordingly. This distribution is more obvious in the most northern core MC 78, and mirrors the north–south decreasing gradient in salinity due to high evaporation rate at the northern Red Sea. Moreover, the $\delta^{18}\text{O}$ of *G. sacculifer* and *G. ruber* becomes heavier relative to the previous and following intervals, reflecting salinity elevation during that time interval. In general, the $\delta^{18}\text{O}$ values of *G. sacculifer* (between -0.11‰ and 0.90‰) are heavier than those of *G. ruber* (between -0.83‰ and 0.36‰), which reflect the slightly deeper habitat of *G. sacculifer*. This interval (4–2 Ky BP) is suggested to be corresponding to the short enhanced arid phase during the Late Holocene in the Red Sea. It is associated with a decrease of northern hemisphere summer insolation, correspondingly, decreasing strength of the African monsoon (e.g. Kutzbach, 1981). As such, the circulation of surface and subsurface water masses and the inflow of Gulf of Aden normal water northward to the Red Sea through the Strait of Bab el Mandeb were reduced. The climatic conditions of the northern Red Sea (no rainfall and river input) which is mainly influenced by dry climate of the Eastern Mediterranean (Mommersteeg et al., 1995), resulted in an enhanced evaporation rate and consequently generate hypersaline water body as reflected from the planktonic foraminiferal species of the studied cores. The transition period spanning the interval 2.5–2 Ky BP has been detected with gradual decreasing trend of salinity. Surface water salinity from about 2 Ky BP to the present seems to be similar, assuming that the present water conditions began to develop immediately after 2 Ky BP. This assumption was deduced from a full establishment of planktonic foraminifera species and the flourishing of species with less salinity tolerance as *G. sacculifer* with the high percentage (over 50%) in the studied cores. *G. sacculifer* reached its level of maximum abundance within a salinity range from about 37‰ to 39‰ (Hemleben et al., 1989). It could be concluded that surface water salinity did not exceed approximately 39‰ during this period of time that is very similar to that of the living assemblage (Weikert, 1987; Siccha et al., 2009). The $\delta^{18}\text{O}$ records suggest the drop in salinity compared to the previous interval. This suggestion was supported by light $\delta^{18}\text{O}$ values of the two index species during this time interval.

Evaluation of paleo-surface water productivity

It has been noticed that the $\delta^{13}\text{C}$ record of *G. sacculifer* is relatively higher than that of *G. ruber*. The $\delta^{13}\text{C}$ of *G. sacculifer* varies between 2.19‰ and 2.86‰ and that of *G. ruber* varies between 1.12‰ and 1.87‰. This result could be related to the different life habitats of the two species within the photic zone. *G. sacculifer* lives closer to the chlorophyll maximum where most of the ^{12}C has been used up compared to *G. ruber* (shallow dwelling species lives higher up) where more ^{12}C is available. This is due to the fact that the plants incorporate more ^{12}C than ^{13}C , thus a phytoplankton-rich region is depleted in ^{12}C and vice versa. In the studied cores, the

4–2 Ky BP interval was characterized by the highest occurrence of *G. ruber*. Despite the fact that the temperature ranges of *G. sacculifer* and *G. ruber* are quite similar, it seems therefore that the abundance of *G. ruber* indicates the relative increase in salinity and trophic conditions. This assumption could be referred to enhanced aridity, consequently, hypersaline; dense surface water favored vertical mixing of the water column. It is worth mentioning that at ~2.5–2 Ky BP, the relative abundance of the four species shows a transitional behavior of the species distribution. This transitional interval represents a period during which changes in the hydrographic conditions of the northern Red Sea might take place and consequently affect the abundance of foraminiferal species. The relative increase in planktonic foraminiferal species during this short transitional period may be related to changes in food supply, migration of foraminifera pursuing food (Hemleben et al., 1987) or due to salinity changes. The short enhanced arid interval (4–2 Ky BP) characterized by elevation of salinity and somewhat productivity, has been followed by a less strength arid period from 2 Ky BP to the present-day. This arid condition was characterized by a maximum relative abundance of *G. sacculifer* and light $\delta^{18}\text{O}$ relative to the previous period. With respect to nutrient level and consequently primary productivity, the Red Sea can be subdivided today at about 18–20°N (Intertropical Convergence Zone, ITCZ) into a more eutrophic in the southern region as monsoon drives nutrient-rich water from the Gulf of Aden and a more oligotrophic in the northern Red Sea due to decrease winter circulation (Edwards, 1987; Haug et al., 2001; Seeberg-Elverfeldt et al., 2004; Fleitmann, 2007). Such a geographic effect is observed in the Red Sea, as the recent planktonic foraminifera mirror the above-mentioned division related to the salinity tolerance and nutritional behavior of the various species. It could be assumed that a period of aridity and oligotrophic conditions in the northern Red Sea exist. The hydrographic condition during that interval is believed to be almost similar to the present time.

Conclusions

High-resolution analysis was carried out on the planktonic foraminiferal fauna of three short cores from the northern Red Sea covering the last 6 Ky indicating that four species (*G. ruber*, *G. sacculifer*, *O. universa* and *G. siphonifera*) are dominant and could be useful as paleo-hydrographic indicators. Arid conditions dominate in the northern Red Sea from about 6 Ky BP to the present and associated with high salinity and oligotrophic conditions. Short enhanced arid phase has been suggested for the time interval between 4 and 2 Ky BP. This interval is characterized by significant elevation of surface water salinity and most likely productivity.

Acknowledgments

Thanks to the ship crew and scientists of R/V Meteor, M 31/2 in 1995. Ch. Hemleben is acknowledged for support and critical discussions in particular for the age model. We are grateful to J. Patzold for his help in the stable isotope analysis at Geosciences Department, Bremen University. Thanks to Ahmed E. Rifaat for reviewing the manuscript.

References

- Abu-Zied, R.H., Basaham, A.S., El Sayed, M.A., 2013. Effect of municipal wastewaters on bottom sediment geochemistry and *Benthic foraminifera* of two Red Sea coastal inlets, Jeddah, Saudi Arabia. *Environ. Earth Sci.* 68, 451–469. <http://dx.doi.org/10.1007/s12665-012-1751-7>.
- Almogi-Labin, A., Hemleben, Ch., Meischner, D., Erlenkeuser, H., 1996. The response of the Red Sea deep-water agglutinated foraminifera to water-mass changes during the late quaternary. *Mar. Micropaleontol.* 28, 283–297.
- Badawi, A., 2015. Late quaternary glacial/interglacial cyclicity models of the Red Sea. *Environ. Earth Sci.* 73 (3), 961–977.
- Badawi, A., Schmiedl, G., Hemleben, Ch., 2005. The impact of late quaternary environmental changes on deep-sea benthic foraminiferal faunas of the Red Sea. *Mar. Micropaleontol.* 58 (1), 13–30.
- Bé, A.W.H., Tolderlund, D.S., 1971. Distribution and ecology of living planktonic foraminifera in surface waters of the Atlantic and Indian Oceans. In: Funnell, M., Riedel, W.R. (Eds.), *Micropaleontology of Oceans*. Cambridge University Press, Cambridge, pp. 105–151.
- Berggren, W.A., Boersma, 1969. Late Pleistocene and Holocene planktonic foraminifera from the Red Sea. In: Degens, E.T., Ross, D.A. (Eds.), *Hot Brines and Recent Heavy Metal Deposits in the Red Sea*. Springer-Verlag, Berlin, pp. 282–299.
- Bijma, J., Faber Jr., W.W., Hemleben, Ch., 1990. Temperature and salinity limits, for growth and survival of some planktonic foraminifera in laboratory cultures. *J. Foramin. Res.* 20, 95–116.
- Birch, H., Coxall, H., Pearson, P., Kroon, D., O'Regan, M., 2013. Planktonic foraminifera stable isotopes and water column structure: disentangling ecological signals. *Mar. Micropaleontol.* 101, 127–145.
- Bower, A.S., Furey, H.H., 2012. Mesoscale eddies in the Gulf of Aden and their impact on the spreading of Red Sea outflow water. *Prog. Oceanogr.* 96, 14–39.
- Cember, R.P., 1988. On the sources, formation and circulation of Red Sea deep water. *J. Geophys. Res.* 93 (C7), 8175–8191.
- Edelman-Fürstenberg, Y., Almog-Labin, A., Hemleben, Ch., 2009. Paleo-oceanographic evolution of the central Red Sea during the Late Holocene. *Holocene* 19 (1), 117–127.
- Edwards, A.J., 1987. Climate and oceanography. In: Edwards, A.J., Head, S.M. (Eds.), *Key Environments: Red Sea*. Pergamon Press, Oxford, pp. 45–70.
- Eshel, G., Naik, N.H., 1997. Climatological coastal jet collision, intermediate water formation, and the general circulation of the Red Sea. *J. Phys. Oceanogr.* 27, 1233–1257.
- Eshel, G., Cane, M.A., Blumenthal, M.B., 1994. Modes of the subsurface, intermediate, and deep-water renewal in the Red Sea. *J. Geophys. Res.* 99, 15941–15952.
- Farmer, E.C., Kaplan, A., deMenocal, P.B., Lynch-Stieglitz, J., 2007. Corroborating ecological depth preferences of planktonic foraminifera in the tropical Atlantic with the stable oxygen isotope ratios of core top specimens. *Paleoceanography* 22 (3) (PA3205).
- Fenton, M., Geiselhart, S., Rohling, E.J., Hemleben, Ch., 2000. A planktonic zones in the Red Sea. *Mar. Micropaleontol.* 40, 277–294.
- Fleitmann, D., 2007. Holocene ITCZ and Indian monsoon dynamics recorded in stalagmites from Oman and Yemen (Socotra). *Quat. Sci. Rev.* 26, 170–188.
- Hamouda, A.Z., 2009. Recent evaluation of the assessment seismic hazards for Nuweiba, Gulf of Aqaba. *Arabian J. Geosci.* <http://dx.doi.org/10.1007/s12517-009-0096-3>.
- Hamouda, A.Z., El-Wahab, M.A., 2009. Sediment characteristics and water circulation of Big Jemsa Bay, Red Sea, Egypt. *Mar. Geophys. Res.* 30, 95–104.

- Hamouda, A.Z., El-Wahab, M.A., 2012. Detection of the bottom facies characteristics at El Zeit Bay, Red Sea, by using a single-beam acoustic sound. *Oceanol. J.* 52, 60–71.
- Haug, G.H., Hughen, K.A., Sigman, D.M., Peterson, L.C., Röhl, U., 2001. Southward migration of the intertropical convergence zone through the Holocene. *Science* 293, 1304–1308.
- Hemleben, Ch., Spindler, M., Breiting, I., Ott, R., 1987. Morphological and physiological responses of *Globigerinoides sacculifer* (Brady) under varying laboratory conditions. *Mar. Micropaleontol.* 12, 305–324.
- Hemleben, Ch., Spidler, M., Anderson, O.R., 1989. *Modern Planktonic Foraminifera*. Springer Verlag, p. 363 pp.
- Hemleben, Ch., Meischner, D., Zahn, R., Almogi-Labin, A., Erlenkeuser, H., Hiller, B., 1996. Three hundred eighty thousand years long stable isotope and faunal record from the Red Sea: influence of global sea level change on hydrography. *Paleoceanography* 11 (2), 147–156.
- Imbrie, J., Hays, J.D., Martinson, D.G., McIntyre, A., Mix, A.C., Morley, J.J., Pisias, N.G., Prell, W.L., Shackleton, N.J., 1984. The orbital theory of Pleistocene climate: support from a reversed chronology of the marine O18 record. In: Berger, A., Imbrie, J., Hays, J., Kugla, G., Satzmann, B. (Eds.), *Milankovitch and Climate*. Riedl, Dordrecht, pp. 269–305.
- Ivanova, E.V., 1985. Late quaternary biostratigraphy and paleotemperatures of the Red Sea and the Gulf of Aden based on planktonic foraminifera and pteropods. *Mar. Micropaleontol.* 9, 335–364.
- Kroon, D., Ganssen, G., 1989. Northern Indian Ocean upwelling cells and the stable isotope compositions of living planktonic foraminifera. *Deep Sea Res.* 36, 1219–1236.
- Kutzbach, J.E., 1981. Monsoon climate of the Early Holocene: climate experiment with the earth's orbital parameters for 9000 years ago. *Science* 214, 59–61.
- Lipps, J.H., 1979. The ecology and paleo-ecology of planktonic foraminifera. In: Lipps, J.H., Berger, W.H., Buzas, M.A., Douglas, R.G., Ross, C.A. (Eds.), *Foraminiferal Ecology and Paleoecology: SEPM Short Course No. 6*, Houston, Texas, pp. 62–104.
- Locke, S.M., Thunell, R.C., 1988. Paleo-oceanographic record of the last glacial/interglacial cycle in the Red Sea and the Gulf of Aden. *Paleogeogr. Palaeoclimatol. Palaeoecol.* 64, 163–187.
- Loeblich, A.R., Tappan, H., 1988. *Foraminiferal Genera and their Classification*. Plates. Van Nostrand Reinhold Company, New York, p. 970 pp.
- Malmgren, B.A., Haq, B.U., 1982. Assessment of qualitative techniques in paleobiogeography. *Mar. Micropaleontol.* 7, 213–236.
- Mommesteeg, H.J.P.M., Loutre, M.F., Young, R., Wijmstra, T.A., Hooghiemstra, H., 1995. Orbital forced frequencies in the 975,000 years pollen record from Tenagi Philippon (Greece). *Clim. Dyn.* 11, 4–24.
- Patzert, W., 1974. The wind-induced reversal in Red Sea circulation. *Deep Sea Res.* 21, 109–121.
- Ravelo, A.C., Fairbanks, R.G., 1992. Oxygen isotopic composition of multiple species of planktonic foraminifera: recorders of the modern photic zone temperature gradient. *Paleoceanography* 7, 815–831.
- Ravelo, A.C., Fairbanks, R.G., 1995. Carbon isotopic fractionation in multiple species of planktonic foraminifera from core-tops in the Tropical Atlantic. *J. Foraminiferal Res.* 25, 53–74.
- Reiss, Z., Luz, B., Almogi-Labin, A., Halicz, E., Winter, A., Wolf, M., Ross, D.A., 1980. Late quaternary paleoceanography of the Gulf of Ababa (Elat), Red Sea. *Quat. Res.* 14, 294–308.
- Rohling, E.J., Sprovieri, M., Cane, T., Casford, J.S.L., Cooke, S., Bouloubassi, I., Emeis, K.C., Schiebel, R., Rogerson, M., Hayes, A., Jorissen, F.J., Kroon, D., 2004. Reconstructing past planktic foraminiferal habitats using stable isotope data: a case history for Mediterranean sapropel S5. *Mar. Micropaleontol.* 50, 89–123.
- Schiebel, R., Hemleben, Ch., 2005. Modern planktic foraminifera. *Paläont. Z.* 79, 135–148.
- Schmiedl, G., Hemleben, Ch., Keller, J., Segl, M., 1998. The impact of climatic changes on the benthic foraminiferal fauna in the Ionian Sea during the last 330,000 years. *Paleoceanography* 13, 447–458.
- Schundnagies, A., Kroon, D., Hemleben, Ch., Van Hinte, J.E., 1990. The distributional pattern of recent pteropods and planktonic foraminifera in surface waters and sediments of the Western Arabian Sea, Gulf of Aden and The Red Sea. *Deep Sea Res. II* 21, 405–424.
- Seeberg-Elverfeldt, I.A., Lange, C.B., Patzold, J., 2004. Preservation of siliceous microplankton in surface sediments of the northern Red Sea. *Mar. Micropaleontol.* 51, 193–211.
- Siccha, M., Trommer, G., Schulz, H., Hemleben, Ch., Kucera, M., 2009. Factors controlling the distribution of planktonic foraminifera in the Red Sea and implications for the development of transfer functions. *Mar. Micropaleontol.* 72, 146–156.
- Siddall, M., Rohling, E.J., Almogi-Labin, A., Hemleben, Ch., Meischner, D., Schmelzer, I., Smeed, D.A., 2003. Sea-level fluctuations during the last glacial cycle. *Nature* 423, 853–858.
- Siddall, M., Smeed, D.A., Hemleben, Ch., Rohling, E.J., Schmelzer, I., Peltier, W.R., 2004. Understanding the Red Sea response to sea level. *Earth Planet. Sci. Lett.* 225, 421–434.
- Smeed, D.A., 2004. Exchange through the Bab el Mandeb. *Deep Sea Res. II* 51, 455–474.
- Vincent, E., Berger, W.H., 1981. Planktonic foraminifera and their use in paleoceanography. In: Emiliani, C. (Ed.), *The Oceanic Lithosphere: The Sea*, vol. 7, New York, pp. 1025–1119 (Chapter 25).
- Weikert, H., 1987. Plankton and the pelagic environment, in the Red Sea. In: Edwards, A.J., Head, S.M. (Eds.), *Key Environments: Red Sea*. Pergamon Press, Oxford, pp. 90–111.
- Woelke, S., Quadfasel, D., 1996. Renewal of deep water in the Red Sea during 1982–1987. *J. Geophys. Res.* 101 (C1), 155–165.